



# New physics searches with B mesons at the ATLAS experiment

Tamsin Nooney



on behalf of the ATLAS collaboration

29<sup>th</sup> April 2015  
DIS2015, Dallas, Texas

# Outline

---

- Introduction
- $B_d^0 \rightarrow K^{*0} \mu^+ \mu^-$
- $B_s^0 \rightarrow \mu^+ \mu^-$
- $B_s^0 \rightarrow J/\psi \varphi$
- Summary

# Introduction

---

- The Standard Model (SM) has explained all experimental observations for decades.
- But is an incomplete model.
- Many possible improvements postulated.
- Two approaches to find new physics:
  - Direct.
  - Indirect: *rare decays*.

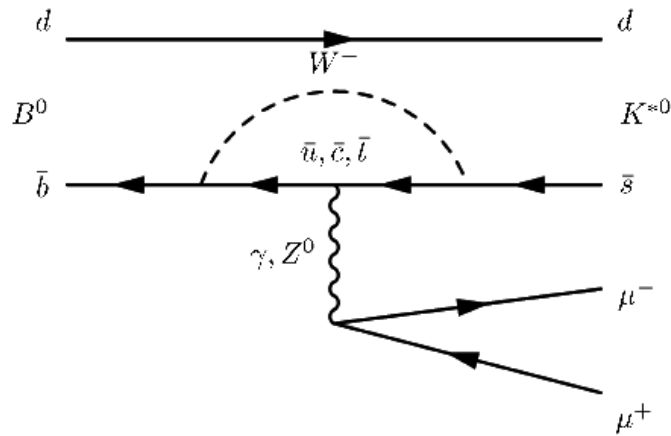


# Angular Analysis of

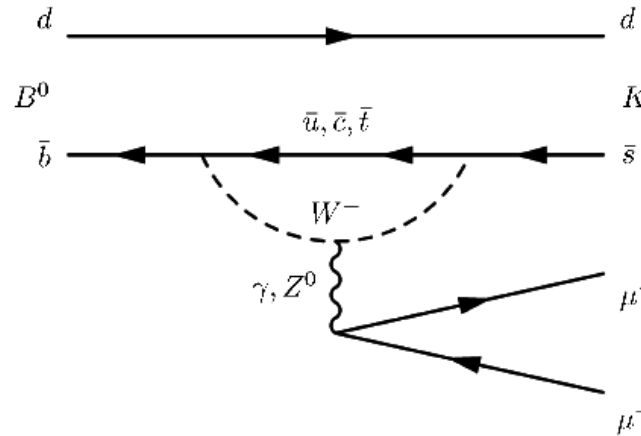
$$B_d^0 \rightarrow K^{*0} \mu^+ \mu^-$$

# Why $B_d^0 \rightarrow K^{*0} \mu^+ \mu^-$ ?

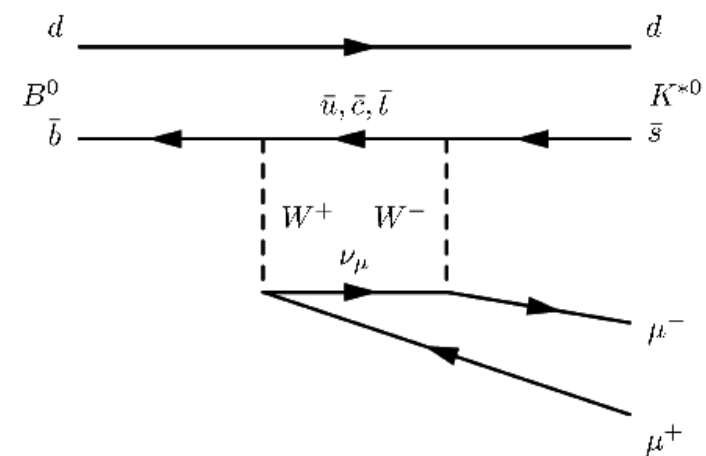
- The (semi-)rare decay  $B_d^0 \rightarrow K^{*0} \mu^+ \mu^-$  is a FCNC decay and thus proceeds via several competing loop diagrams in the SM, allowing for substantial *new physics* contributions.



SM electromagnetic penguin diagram.



SM weak penguin diagram.



SM box diagram.

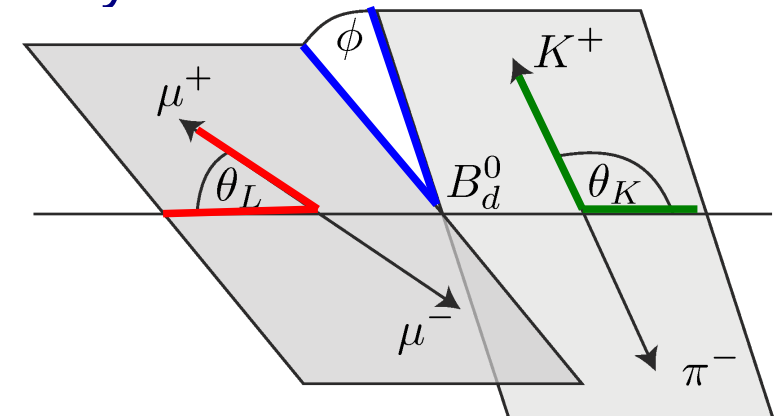
- ➔ Able to test the SM (QCD, effective theories etc.)
- ➔ We can indirectly search for new physics at scales beyond the reach of the LHC.
- ➔ Heightened interest from  $P'_5$  discrepancy. [LHCb-CONF-2015-002]

# What Are We Measuring?

- The decay  $B_d^0 \rightarrow K^{*0} \mu^+ \mu^-$ , where  $K^{*0} \rightarrow K^+ \pi^-$ , is described by **four** kinematic variables:

1) The invariant mass squared  $q^2$  of the dimuon system.

- 2)  $\theta_L$  } Three angles describing the  
3)  $\theta_K$  } geometrical configuration of the  
4)  $\phi$  } final state as shown.



- The angular distribution is factorised in terms of the helicity angle distributions according to a chosen **angular PDF** and any **observables** of interest are extracted.

# 2011 Formalism

- At a given  $q^2$  the integration of the differential decay rate over  $\theta_K$  and  $\varphi$  gives:

$$\frac{1}{\Gamma} \frac{d^2\Gamma}{d\cos\theta_\ell dq^2} = \frac{3}{4} F_L(q^2) (1 - \cos^2\theta_\ell) + \frac{3}{8} (1 - F_L(q^2)) (1 + \cos^2\theta_\ell) + A_{FB}(q^2) \cos\theta_\ell,$$

and over  $\theta_L$  and  $\varphi$  gives:

$$\frac{1}{\Gamma} \frac{d^2\Gamma}{d\cos\theta_K dq^2} = \frac{3}{2} F_L(q^2) \cos^2\theta_K + \frac{3}{4} (1 - F_L(q^2)) (1 - \cos^2\theta_K).$$

$F_L(q^2)$  is the longitudinal polarisation of the  $K^{*0}$ .

$A_{FB}(q^2)$  is the forward-backward asymmetry of the muons.

- We fit  $f(\cos\theta_L)f(\cos\theta_K)$  to improve the precision on  $F_L$ , but also introduces a small bias on that quantity.

# Analysis Strategy

---

## ■ Trigger:

Two muon candidates with opposite charge.

## ■ Background:

Combinatorial from  $b\bar{b} \rightarrow \mu^+ \mu^- X$ ,  $c\bar{c} \rightarrow \mu^+ \mu^- X$ , Drell Yan.  
Resonant from exclusive decay channels.

Remove radiative charmonium decays from B decays:



## ■ Cuts:

Optimised by maximising the estimator:

$$P(N_{\text{sig}}, N_{\text{bckg}}) = N_{\text{sig}} / \sqrt{(N_{\text{sig}} + N_{\text{bckg}})}$$

## ■ Mass region:

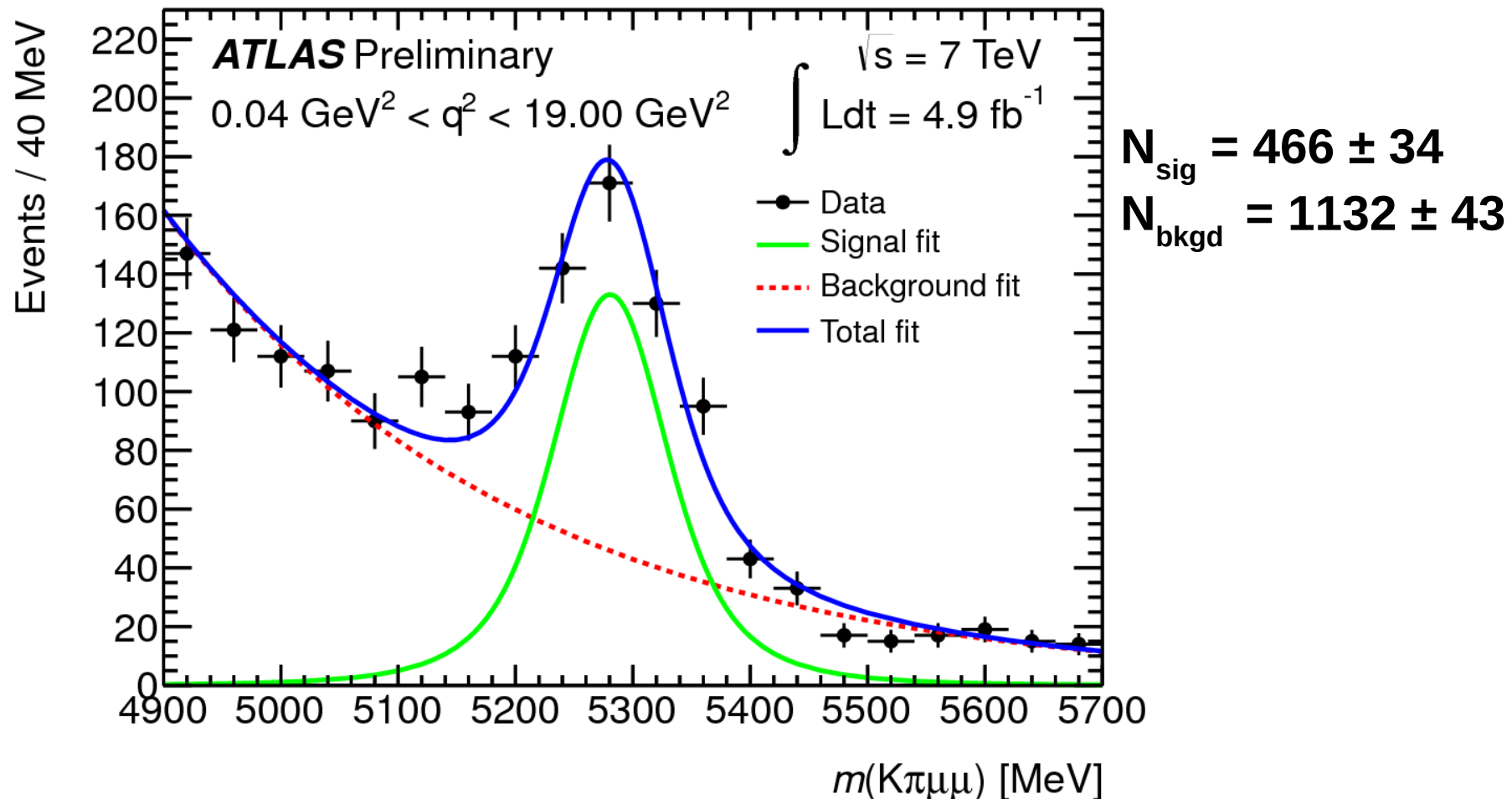
$$4600 \text{ MeV} < m(K\pi\mu\mu) < 5900 \text{ MeV}$$

→ 4466 candidates in the full  $q^2$  range, after the optimised selection.



# ATLAS 2011 Results

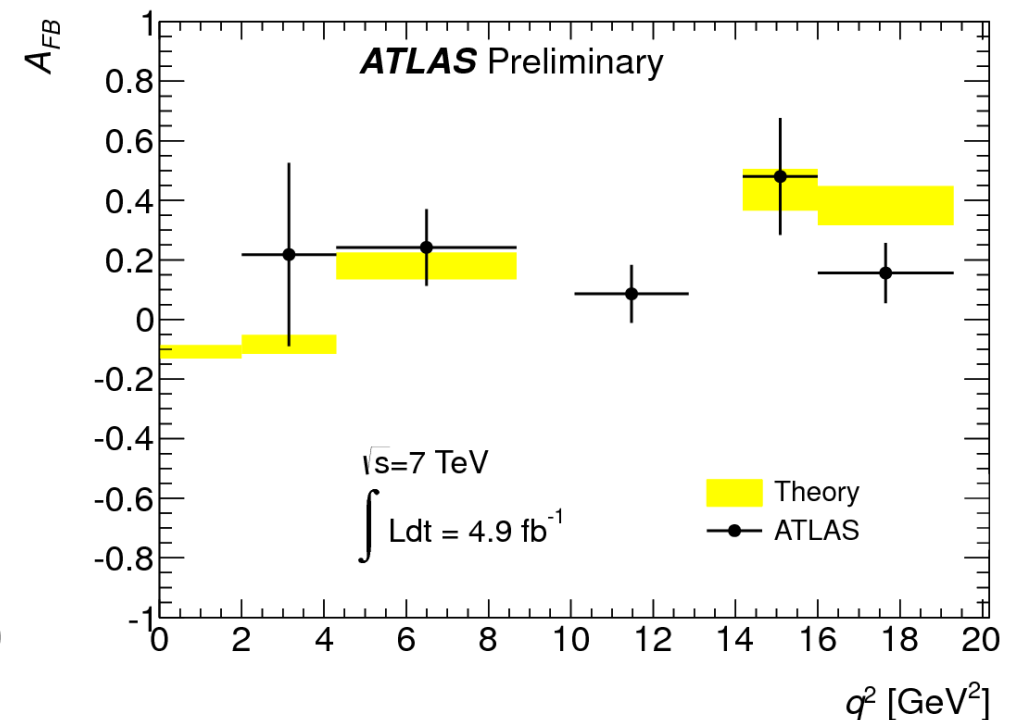
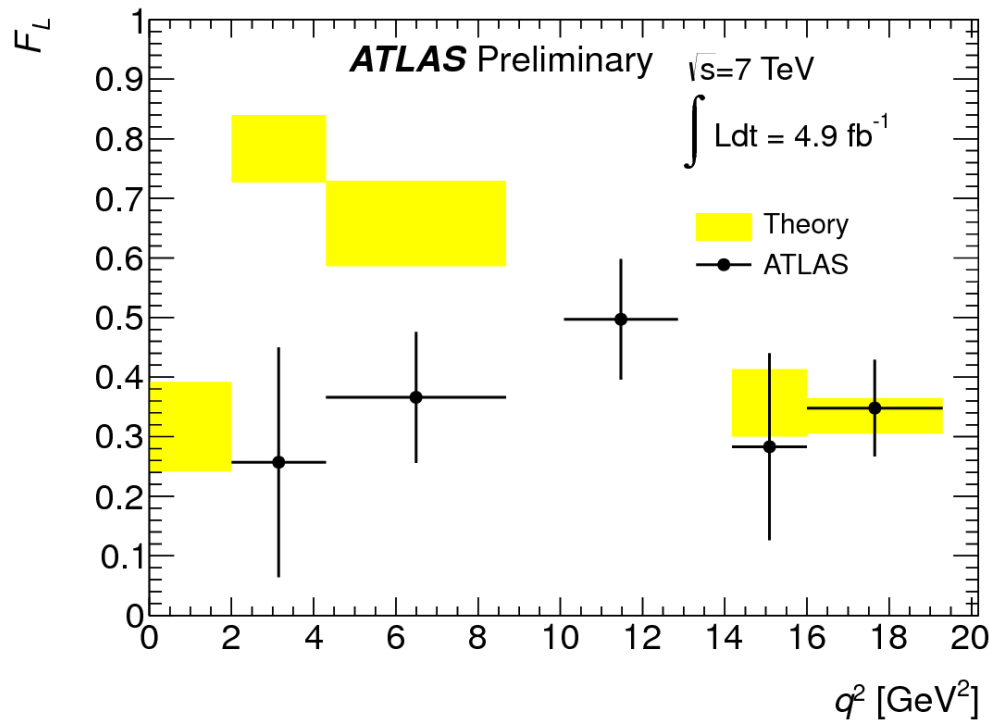
- Invariant mass distribution of  $B_d^0 \rightarrow K^{*0} \mu^+ \mu^-$  candidates after full signal selection using  $4.9 \text{ fb}^{-1}$  of data:



# ATLAS 2011 Results

- Total signal event yield of 454.
- The angular observables are consistent with the SM.  
[C. Bobeth et al. arXiv:1105.2659].

$q^2$ range (GeV <sup>2</sup> )	$N_{sig}$	$A_{FB}$	$F_L$
$2.00 < q^2 < 4.30$	$19 \pm 8$	$0.22 \pm 0.28 \pm 0.14$	$0.26 \pm 0.18 \pm 0.06$
$4.30 < q^2 < 8.68$	$88 \pm 17$	$0.24 \pm 0.13 \pm 0.01$	$0.37 \pm 0.11 \pm 0.02$
$10.09 < q^2 < 12.86$	$138 \pm 31$	$0.09 \pm 0.09 \pm 0.03$	$0.50 \pm 0.09 \pm 0.04$
$14.18 < q^2 < 16.00$	$32 \pm 14$	$0.48 \pm 0.19 \pm 0.05$	$0.28 \pm 0.16 \pm 0.03$
$16.00 < q^2 < 19.00$	$149 \pm 24$	$0.16 \pm 0.10 \pm 0.03$	$0.35 \pm 0.08 \pm 0.02$
$1.00 < q^2 < 6.00$	$42 \pm 11$	$0.07 \pm 0.20 \pm 0.07$	$0.18 \pm 0.15 \pm 0.03$



29/04/15

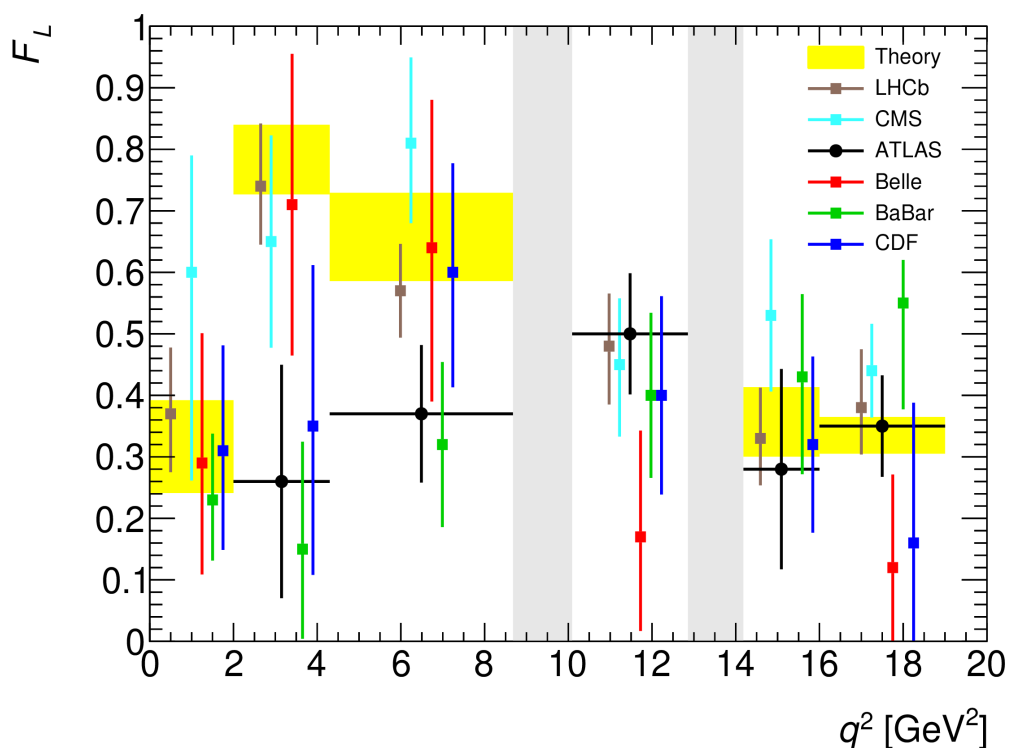
Tamsin Nooney, DIS2015

$$B_d^0 \rightarrow K^{*0} \mu^+ \mu^-$$

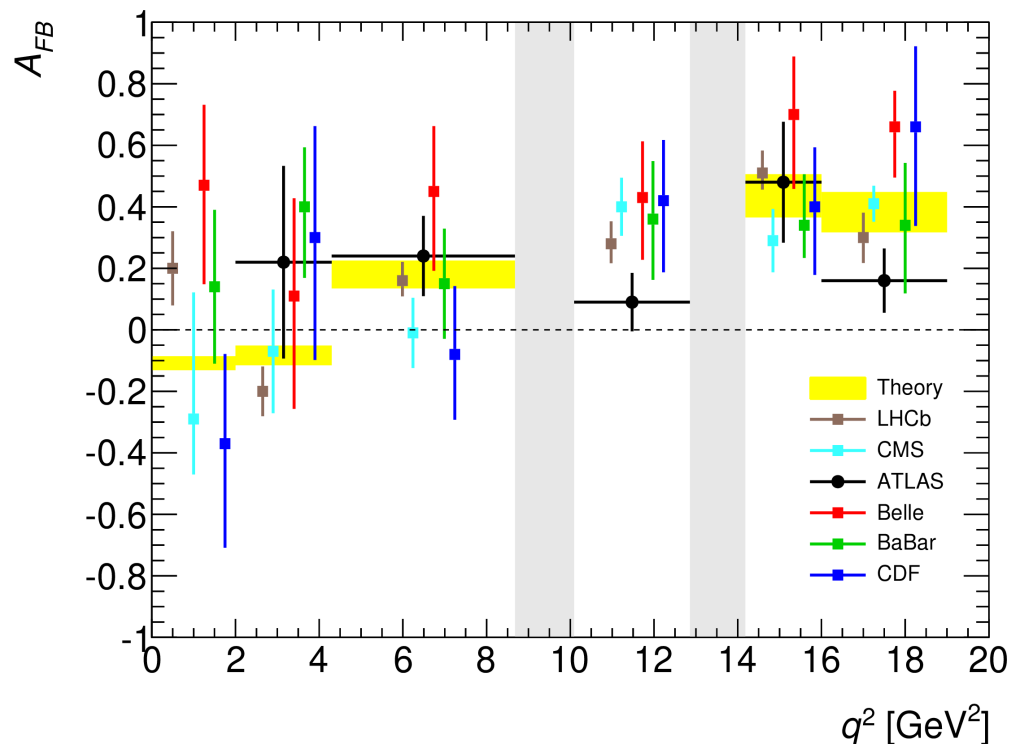
10

# 2011 Results

- $F_L$  and  $A_{FB}$  as a function of  $q^2$  measured by ATLAS (black dots) with the results of other experiments shown in conjunction.



Theory [Phys. Rev. D 87 (2013) 034016]  
 LHCb [JHEP 1308 (2013) 131]  
 BaBar [arXiv:1301.1700v1]  
 CDF [Phys. Rev. Lett., 108 (2012) 081807]

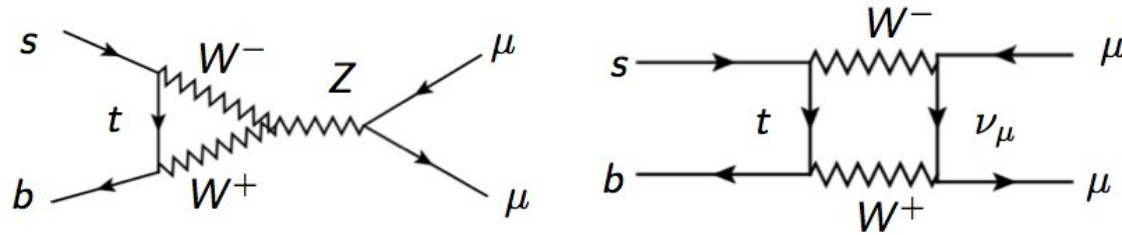


ATLAS [ATLAS-CONF-2013-038]  
 CMS [Phys. Lett. B, 727 (2013) 77-100]  
 Belle [Phys. Rev. Lett., 103 (2009) 171801]

# Search for $B_s^0 \rightarrow \mu^+ \mu^-$ decay

# Why $B_s^0 \rightarrow \mu^+ \mu^-$ ?

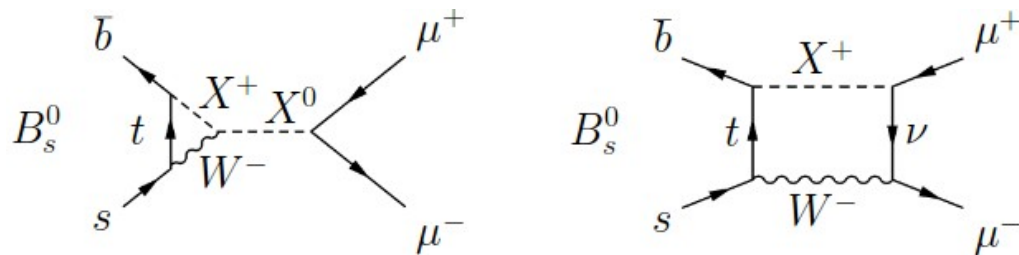
- FCNC, highly suppressed in the SM.



- Very precise SM branching ratio predictions:

$$\mathcal{B}(B_s^0 \rightarrow \mu^+ \mu^-) = (3.66 \pm 0.23) \times 10^{-9}, \text{ compatible at } 1.2\sigma.$$

- Coupling to non-SM particles in competing diagrams can affect the branching ratio.



[Bobeth et al., PRL 112 (2014) 101801]

- Combined CMS and LHCb dataset:

$$\mathcal{B}(B_s^0 \rightarrow \mu^+ \mu^-) = (2.79^{+0.66+0.26}_{-0.60-0.19}) \times 10^{-9}, \text{ } 6.2\sigma \text{ observed (} 7.6\sigma \text{ expected)}$$

# $B_s^0 \rightarrow \mu^+ \mu^-$ 2011 Measurement

- The branching fraction ( $\mathcal{B}$ ) can be written as:

[LHCb: JHEP 1304 (2013) 001]

$$\mathcal{B}(B_S \rightarrow \mu^+ \mu^-) = \underbrace{\mathcal{B}(B^\pm \rightarrow J/\psi K^\pm \rightarrow \mu^+ \mu^- K^\pm)}_{\text{[PDG 2012]}} \cdot \frac{f_u}{f_s} \cdot \frac{\epsilon_{J/\psi K^\pm} \cdot A_{J/\psi K^\pm}}{\epsilon_{\mu^+ \mu^-} \cdot A_{\mu^+ \mu^-}} \cdot \frac{N_{\mu^+ \mu^-}}{N_{J/\psi K^\pm}}$$

Data-calibrated MC  
 $\epsilon \cdot A = N_{\text{rec+sel}} / N_{\text{gen}}$

- Reference channel  $B^\pm \rightarrow J/\psi (\mu^+ \mu^-) K^\pm$  (which introduces partial cancelation of systematic errors.)

Channel	Signal region	Sideband regions
$B_s^0 \rightarrow \mu^+ \mu^-$	[5066, 5666] MeV	[4766, 5066] MeV [5666, 5966] MeV
$B^\pm \rightarrow J/\psi K^\pm$	[5180, 5380] MeV	[4930, 5130] MeV [5430, 5630] MeV

- Blind analysis  $\rightarrow$  invariant mass region  $\pm 300$  MeV around  $B_s^0$  mass.
- Count events  $N_{\mu^+ \mu^-}$  in signal region.

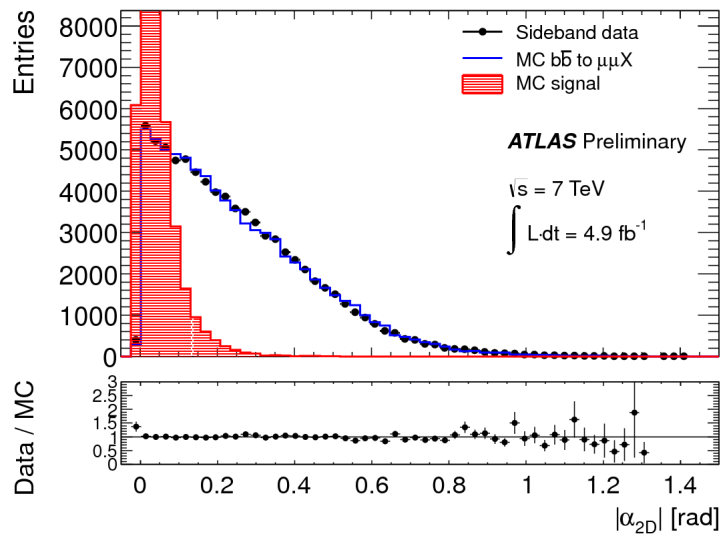
# Analysis Strategy

## Background discrimination

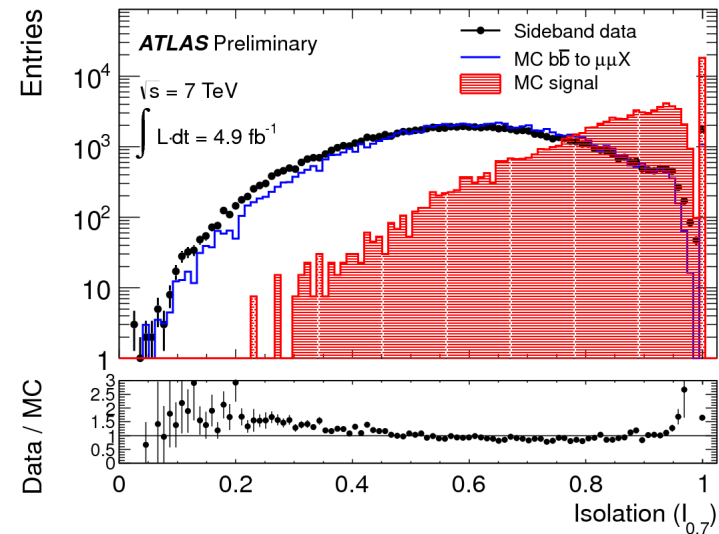
ATLAS-CONF-2013-076

- Boosted Decision Tree (BDT) used (13 discriminating variables).
- Continuum dominated by  $b\bar{b} \rightarrow \mu^+ \mu^- X$ .
- Resonant background due to fake muons, dominated by  $B \rightarrow hh$ .
- Odd numbered events from sidebands used for BDT cut optimisation.
- Even numbered events from sidebands used for interpolation.

### Pointing angle



### Isolation



## BDT selection

29/04/15

Tamsin Nooney, DIS2015

15

$$B_s^0 \rightarrow \mu^+ \mu^-$$

# Analysis Strategy

## Background discrimination

ATLAS-CONF-2013-076

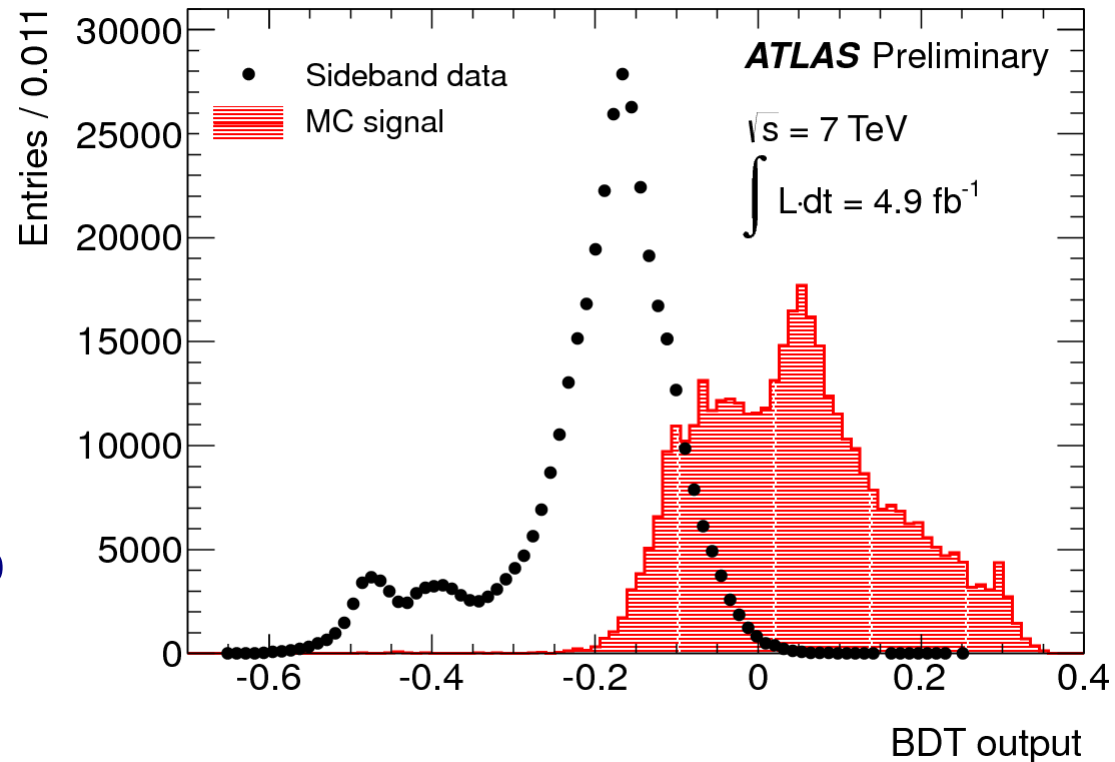
## BDT selection

- Selection optimisation:  
**q**: BDT event classifier  
 **$\Delta m$** : signal mass window width

- Maximise estimator:

$$P(\Delta m, q) = \frac{\epsilon_{\text{sig}}}{1 + \sqrt{N_{\text{bkg}}}}$$

- $P_{\text{max}} = 0.0145$ . Corresponding to final selection cuts:  
 $q > 0.118$   
 $\Delta m = 121 \text{ MeV}$





# $B_s^0 \rightarrow \mu^+ \mu^-$ 2011 Result

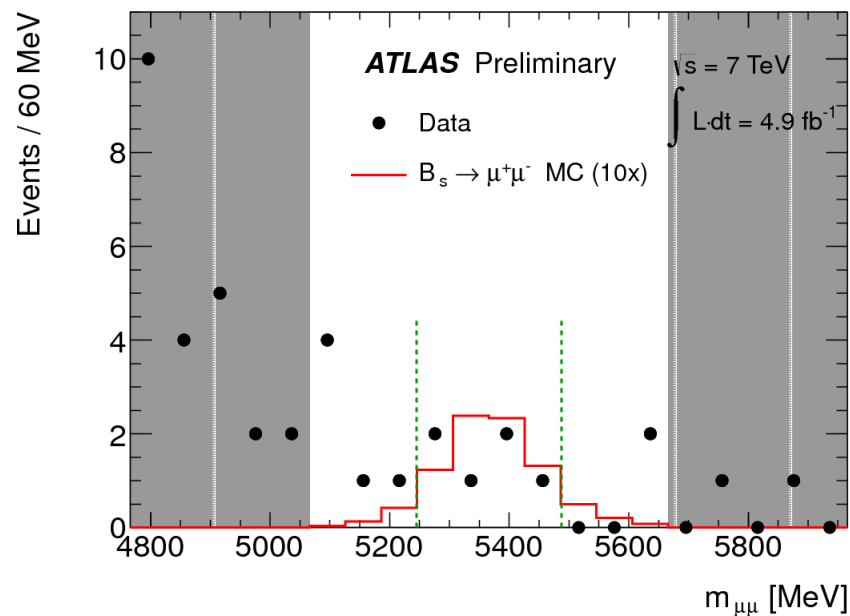
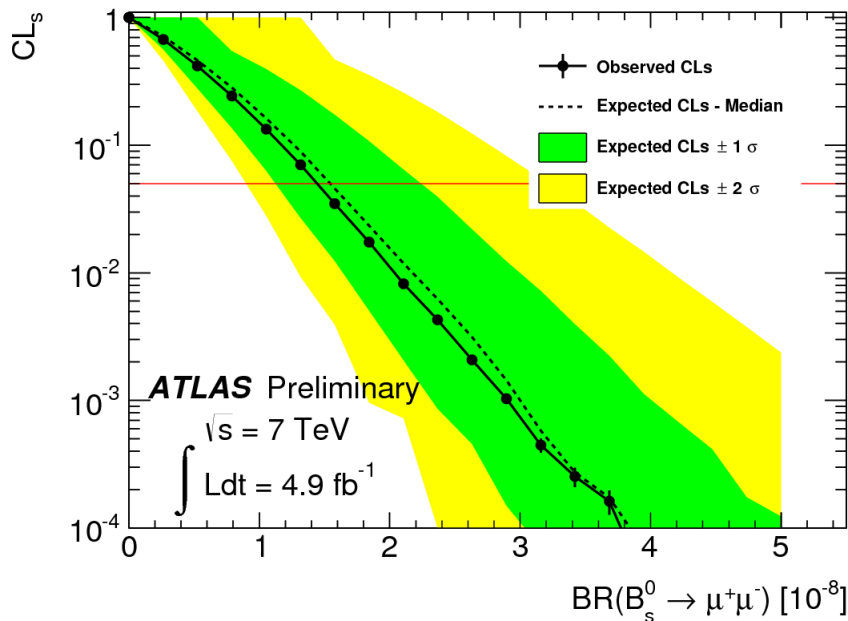
- Single-event-sensitivity (SES) defined as the  $\mathcal{B}$  given by 1 observed event:

$$\text{SES} = \mathcal{B}(B^\pm \rightarrow J/\psi K^\pm \rightarrow \mu^+ \mu^- K^\pm) \cdot \frac{f_u}{f_s} \cdot \frac{\epsilon_{J/\psi K^\pm} \cdot A_{J/\psi K^\pm}}{\epsilon_{\mu^+ \mu^-} \cdot A_{\mu^+ \mu^-}} \cdot \frac{1}{N_{J/\psi K^\pm}} = (2.07 \pm 0.26) \cdot 10^{-9}$$

- SES systematic = 12.5 % (dominated by reference channel  $\mathcal{B}$ ,  $f_u/f_s$  &  $A \cdot \epsilon$ )

$\mathcal{B}(B_s^0 \rightarrow \mu^+ \mu^-) < 1.5 (1.2) \times 10^{-8}$  at 95% (90%) CL

ATLAS-CONF-2013-076

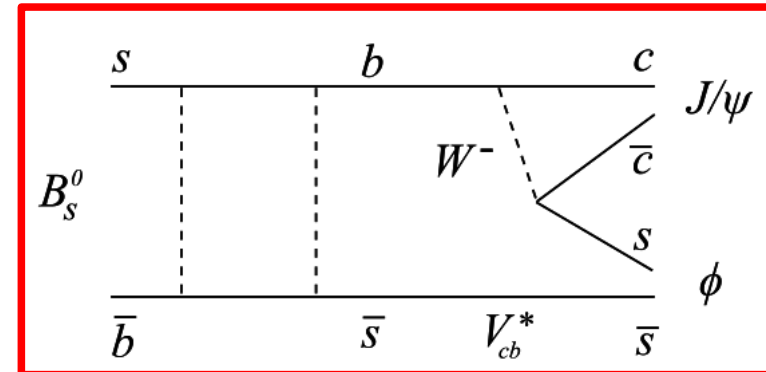
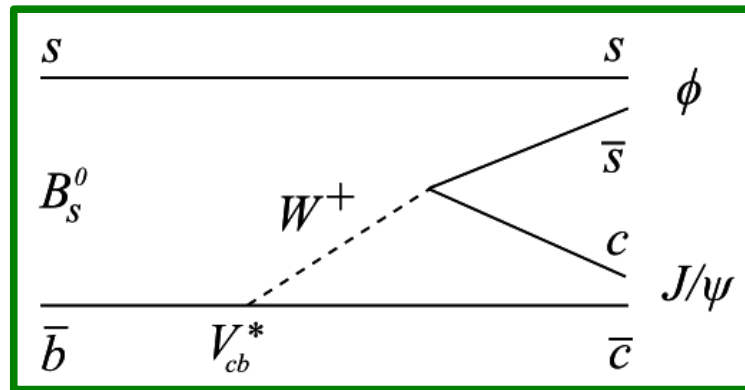


$N_{\text{expBkg}} = 6.7$   
 $N_{\mu^+ \mu^-} = 6$

# Flavour tagged time-dependent angular analysis of $B^0_s \rightarrow J/\psi \phi$

# Why $B_s^0 \rightarrow J/\psi \phi$ ?

- Expected to be sensitive to BSM physics.
- CP violation occurs due to interference between **direct decays** and decays with  $B_s^0 - \bar{B}_s^0$  **mixing** (oscillation frequency characterized by  $\Delta m_s$  between  $B_H$  and  $B_L$ ).



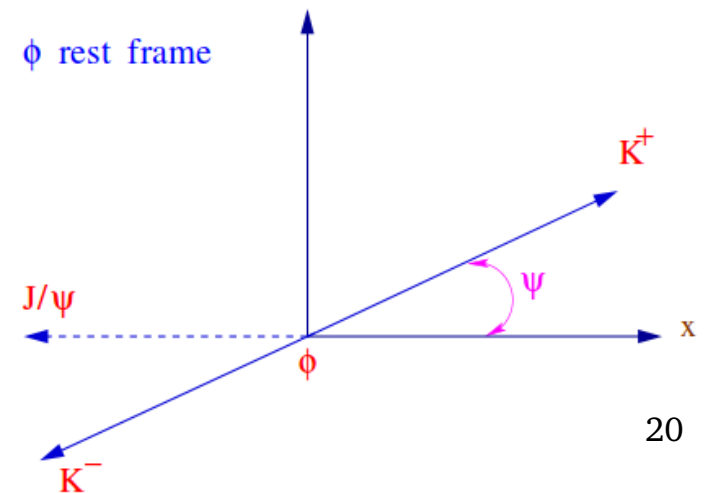
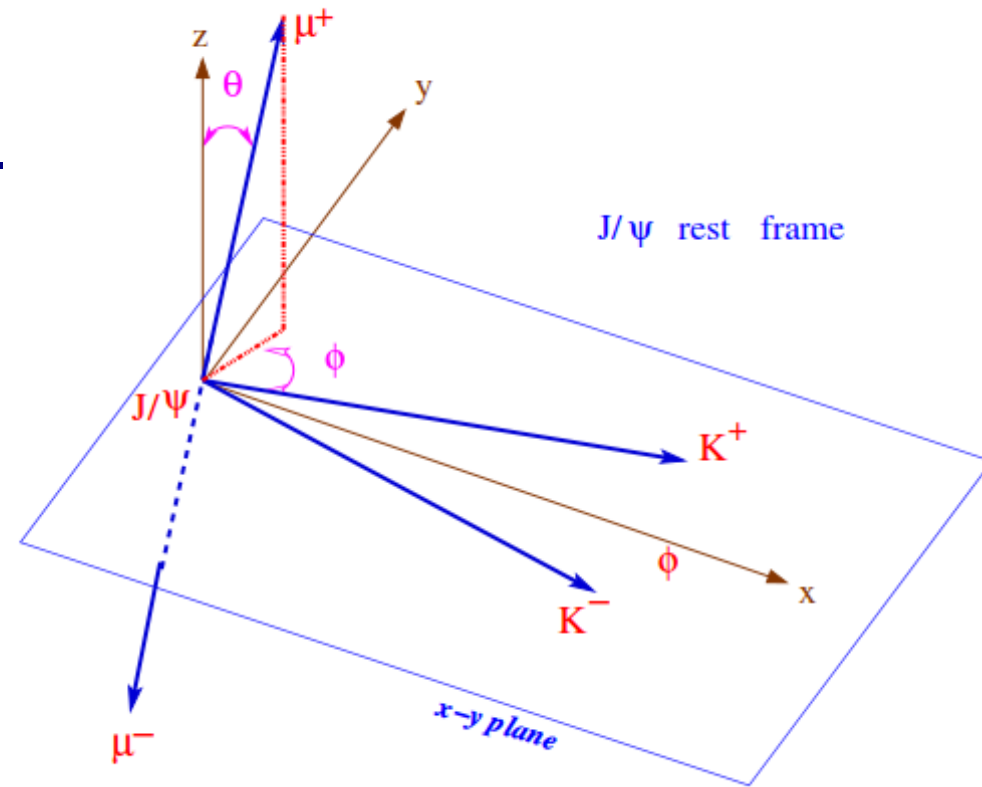
- CP-violating weak phase difference  $\varphi_s$  is precisely predicted in SM:  
 $\varphi_s = -0.037 \pm 0.002 \text{ rad}$  [Phys. Rev. Lett. 97,151803 (2006).]
- SM also predicts decay width difference:  
 $\Delta\Gamma_s = 0.087 \pm 0.021 \text{ ps}^{-1}$  [arXiv:1102.4274]

# Measurement

- Pseudoscalar  $\rightarrow$  vector vector decay.
- Admixture of CP odd ( $L = 1$ ) and CP even ( $L = 0, 2$ ) states.
- Flavor tagging is used to distinguish between the initial  $B_s^0$  and  $\bar{B}_s^0$  states.
- Time-dependent angular analysis to resolve CP eigenstates.

$$\frac{d^4\Gamma}{dt d\Omega} = \sum_{k=1}^{10} \mathcal{O}^{(k)}(t) g^{(k)}(\theta_T, \psi_T, \phi_T)$$

- Unbinned maximum likelihood fit performed on selected events.



# Analysis Strategy

PHYSICAL REVIEW D 90, 052007 (2014)

- Triggers on  $J/\psi \rightarrow \mu^+ \mu^-$  decay.
- Opposite side tagging (OST) used to determine initial flavour of neutral B meson (calibrated using  $B^\pm \rightarrow J/\psi K^\pm$ ).

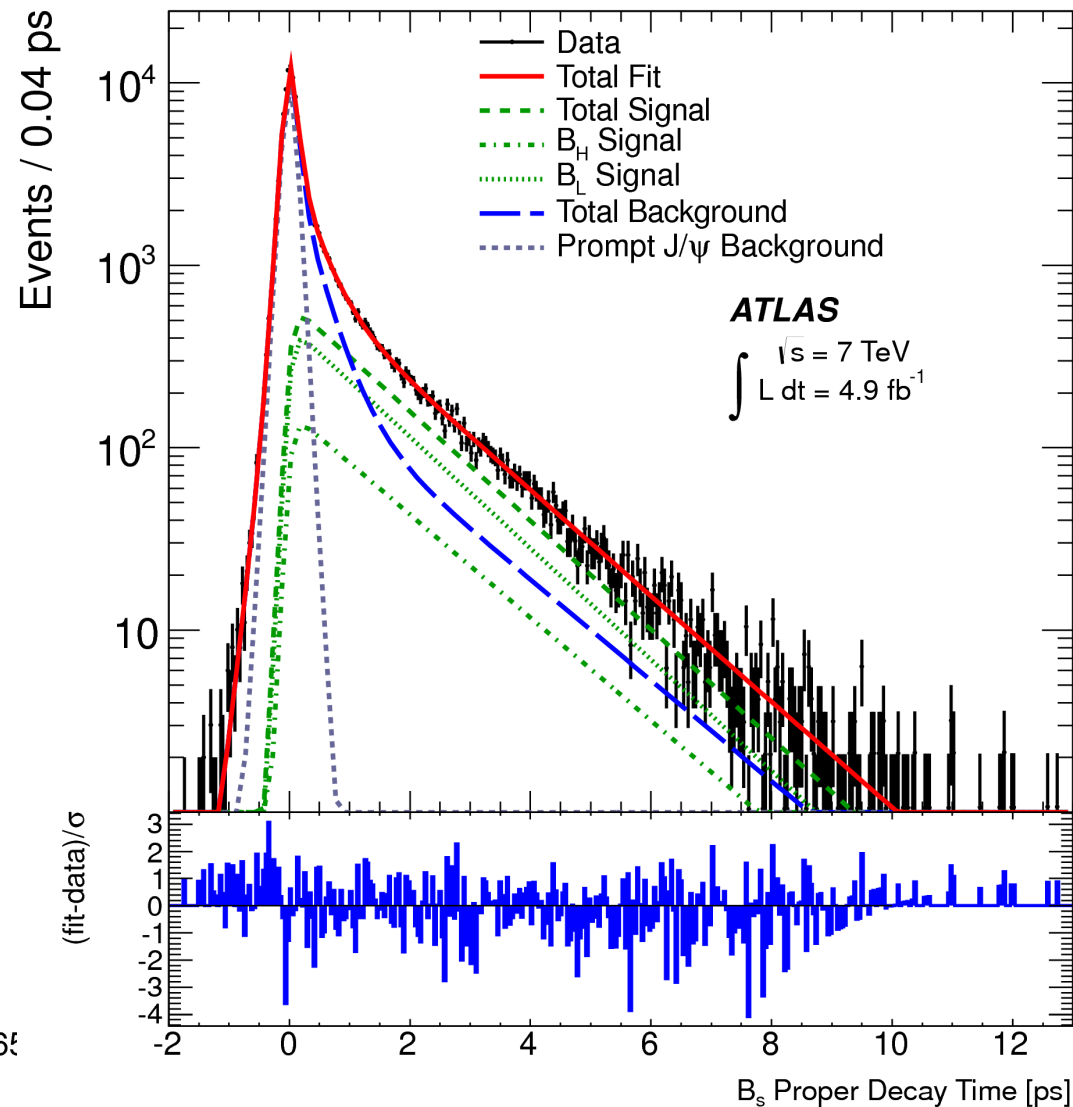
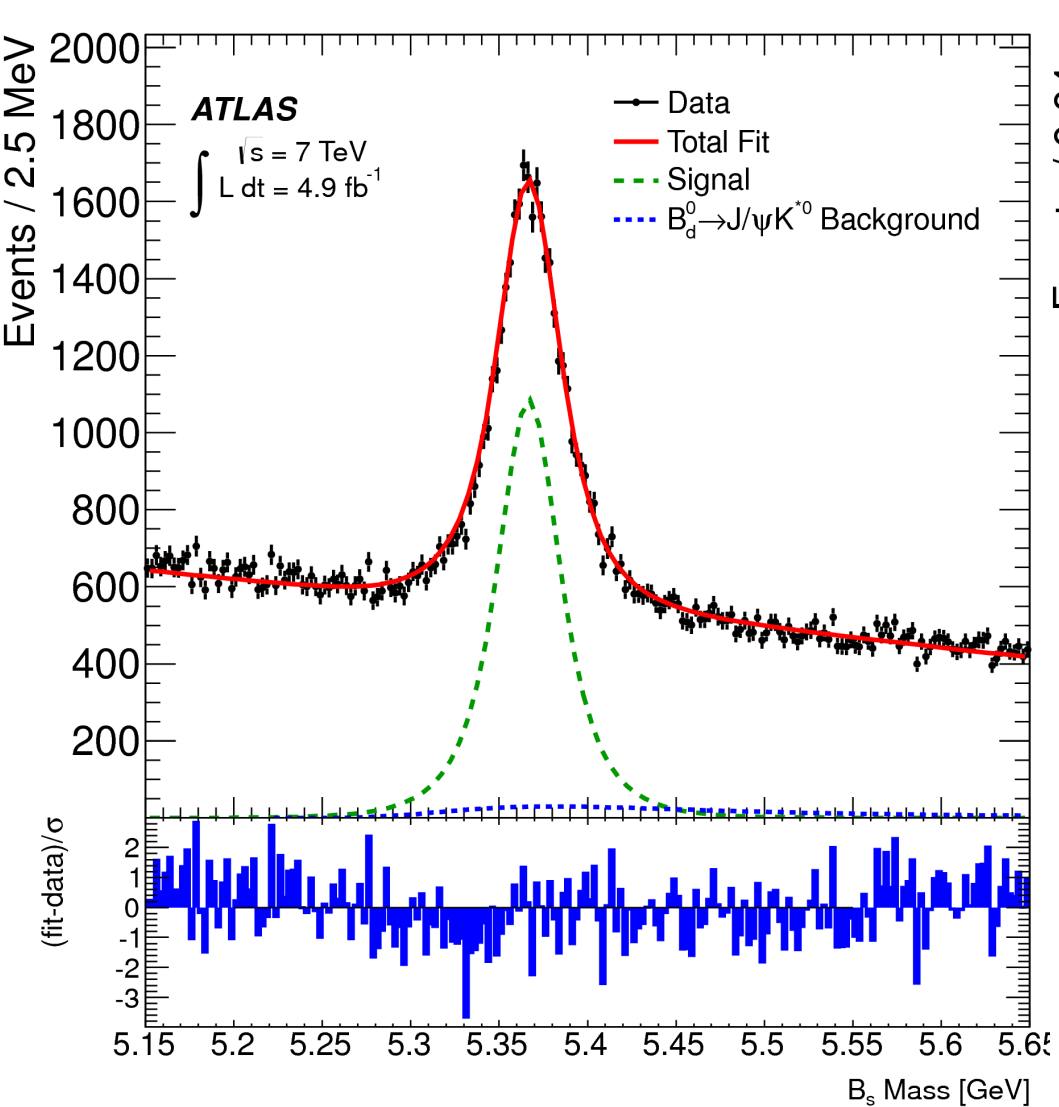
Tagger	Efficiency (%)	Dilution (%)	Tagging power (%)
Combined $\mu$	$3.37 \pm 0.04$	$50.6 \pm 0.5$	$0.86 \pm 0.04$
Segment tagged $\mu$	$1.08 \pm 0.02$	$36.7 \pm 0.7$	$0.15 \pm 0.02$
Jet charge	$27.7 \pm 0.1$	$12.68 \pm 0.06$	$0.45 \pm 0.03$
Total	$32.1 \pm 0.1$	$21.3 \pm 0.08$	$1.45 \pm 0.05$

→ **131513  $B_s^0$**   
**candidates within**  
**a mass range of**  
 **$5.15 \text{ GeV} < m(B_s^0)$**   
 **$< 5.65 \text{ GeV}$**

- Two  $B_d^0$  background channels:  $B_d^0 \rightarrow J/\psi(\mu^+ \mu^-) K^+ \pi^-$   
 $B_d^0 \rightarrow J/\psi(\mu^+ \mu^-) K^{*0} (K^+ \pi^-)$
- Combinatorial background
- $B_s^0 \rightarrow J/\psi(\mu^+ \mu^-) \varphi(K^+ K^-)$  signal PDF extracted,  $f(m, t, \Omega, P(B|Q))$
- Two S-wave signal channels:  
 non-resonant  $B_s^0 \rightarrow J/\psi(\mu^+ \mu^-) K^+ K^-$   
 resonant  $B_s^0 \rightarrow J/\psi(\mu^+ \mu^-) f_0(K^+ K^-)$

# ATLAS 2011 Result

PHYSICAL REVIEW D 90, 052007 (2014)

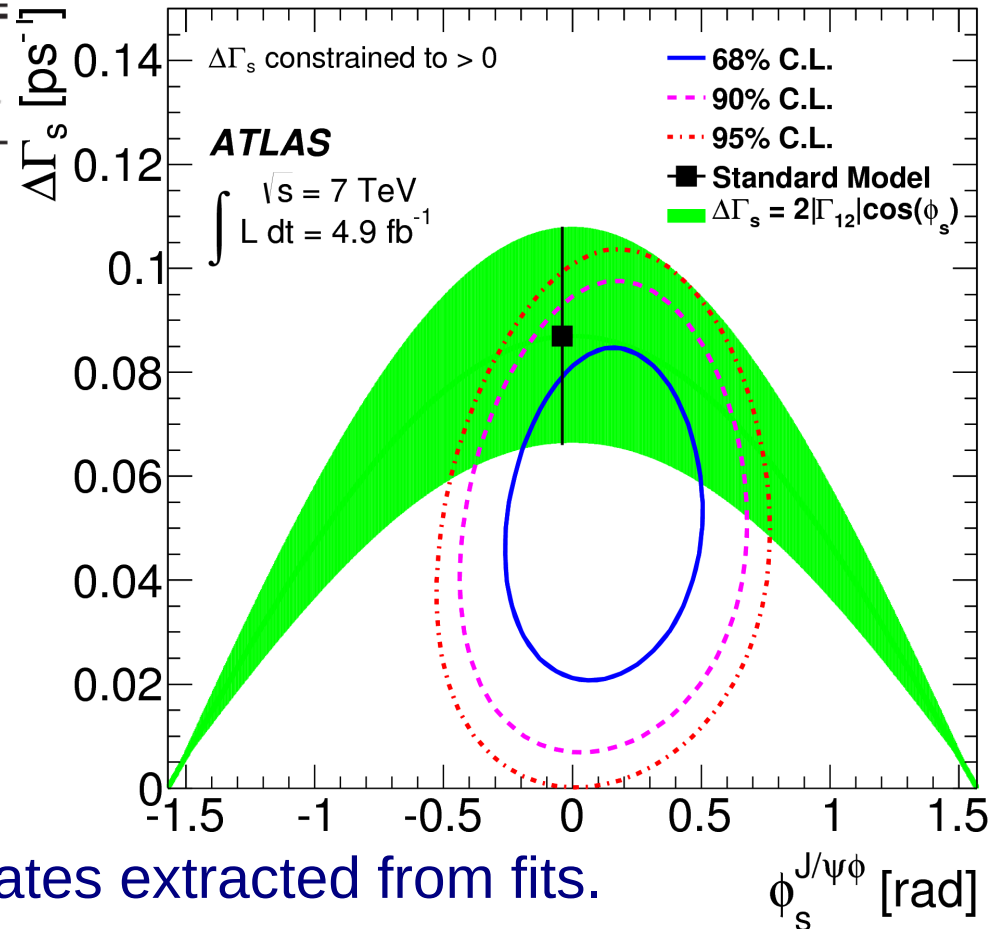


# ATLAS 2011 Result

- Fitted  $B_s^0 \rightarrow J/\psi \phi$  decay parameters and their uncertainties using 4.9  $\text{fb}^{-1}$  of data:

PHYSICAL REVIEW D 90, 052007 (2014)

Parameter	Value	Statistical uncertainty	Systematic uncertainty
$\phi_s$ [rad]	0.12	0.25	0.05
$\Delta\Gamma_s$ [ $\text{ps}^{-1}$ ]	0.053	0.021	0.010
$\Gamma_s$ [ $\text{ps}^{-1}$ ]	0.677	0.007	0.004
$ A_{\parallel}(0) ^2$	0.220	0.008	0.009
$ A_0(0) ^2$	0.529	0.006	0.012
$ A_{\perp}(0) ^2$	0.024	0.014	0.028
$\delta_{\perp}$	3.89	0.47	0.11
$\delta_{\parallel}$	[3.04, 3.23]		0.09
$\delta_{\perp} - \delta_{\parallel}$	[3.02, 3.25]		0.04



Transversity amplitudes

Strong phases (68% CL)

- 22670  $\pm$  150 signal  $B_s^0$  meson candidates extracted from fits.
- Consistent with values obtained in untagged analysis.
- Consistent with the values predicted in the SM.

# Summary

---

- $B_d^0 \rightarrow K^{*0} \mu^+ \mu^-$ 
  - Measurement of  $F_L$  and  $A_{FB}$  using  $4.9 \text{ fb}^{-1}$  of data presented.
  - Mostly consistent with SM.
  - 2012 analysis ongoing.
  - Plan to move towards an optimised observable parameterisation.
- $B_s^0 \rightarrow \mu^+ \mu^-$ 
  - Upper limit on branching fraction set, using  $4.9 \text{ fb}^{-1}$  of data.
  - Consistent with SM.
  - 2012 analysis ongoing, expect to unblind soon.
- $B_s^0 \rightarrow J/\psi \phi$ 
  - Flavour-tagging analysis performed on  $4.9 \text{ fb}^{-1}$  of data.
  - Decay parameters including  $\phi_s$  and  $\Delta\Gamma_s$  presented.
  - Results consistent with SM expectations.
  - Expect updated analysis using 2012 data to be out soon.



# Back Up

**$B_d^0 \rightarrow K^{*0} \mu^+ \mu^-$  Back Up**

# Traditional Angular Analysis

- Traditional full angular analysis of the data using:

$$\frac{1}{\Gamma} \frac{d^5\Gamma}{d \cos \theta_l d \cos \theta_K d\phi dq^2} = \frac{9}{16\pi} \left\{ \left( \frac{2F_S(q^2)}{3} + \frac{4A_S(q^2)}{3} \cos \theta_K (1 - \cos^2 \theta_L) \right) \right. \\ + (1 - F_S(q^2)) \left[ \frac{2F_L(q^2)}{3} \cos^2 \theta_K (1 - \cos^2 \theta_L) + \frac{1 - F_L(q^2)}{2} (1 - \cos^2 \theta_K)(1 + \cos^2 \theta_L) \right. \\ + \frac{1 - F_L(q^2)}{2} \frac{A_T^2(q^2)}{3} (1 - \cos^2 \theta_K)(1 - \cos^2 \theta_L) \cos 2\phi \\ + \frac{4A_{FB}(q^2)}{3} (1 - \cos^2 \theta_K) \cos \theta_L \\ \left. \left. + \frac{A_{Im}(q^2)}{3} (1 - \cos^2 \theta_K)(1 - \cos^2 \theta_L) \sin 2\phi \right] \right\}$$

- Can add a scalar component to the fit introducing two new parameters.
- The full distribution introduces two additional parameters to extract.
- 6 observables of interest are:  $F_L$ ,  $A_{FB}$ ,  $F_S$ ,  $A_S$ ,  $A_T$ ,  $A_{im}$ .

✓ Complete information.

x FF dependent observables at leading order.

# Optimised Observable Analysis

- FF independent analysis:

$$\begin{aligned} \frac{1}{(\Gamma + \bar{\Gamma})} \frac{d^4(\Gamma + \bar{\Gamma})}{d \cos \theta_l d \cos \theta_K d \phi d q^2} = & \frac{9}{32\pi} \left[ \frac{3}{4} (1 - F_L) \sin^2 \theta_K + F_L \cos^2 \theta_K \right. \\ & + \frac{1}{4} (1 - F_L) \sin^2 \theta_K \cos 2\theta_l - F_L \cos^2 \theta_K \cos 2\theta_l \\ & + S_3 \sin^2 \theta_K \sin^2 \theta_l \cos 2\phi + S_4 \sin 2\theta_K \sin 2\theta_l \cos \phi \\ & + S_5 \sin 2\theta_K \sin \theta_l \cos \phi + S_6 \sin^2 \theta_K \cos \theta_l + S_7 \sin 2\theta_K \sin \theta_l \sin \phi \\ & \left. + S_8 \sin 2\theta_K \sin 2\theta_l \sin \phi + S_9 \sin^2 \theta_K \sin^2 \theta_l \sin 2\phi \right]. \end{aligned}$$

- In addition to  $F_L$ , we can measure the FF independent parameters.

$$P_i^{(s,c)} = \frac{S_i^{(s,c)}}{\sqrt{F_L(1 - F_L)}}$$

→ 9 observables to measure in total.

- Can reduce the number of observables directly by **folding** the differential decay rate and exploiting the symmetries in the angular expressions, e.g.:

$$\begin{aligned} \phi & \rightarrow -\phi \quad \text{if } \phi < 0 \\ \theta_l & \rightarrow \pi - \theta_l \quad \text{if } \theta_l > \frac{\pi}{2} \end{aligned}$$

# Optimised Observable Analysis

- We will perform a FF independent analysis:

$$\begin{aligned} \frac{1}{(\Gamma + \bar{\Gamma})} \frac{d^4(\Gamma + \bar{\Gamma})}{d \cos \theta_l d \cos \theta_K d \phi d q^2} = & \frac{9}{32\pi} \left[ \frac{3}{4} (1 - F_L) \sin^2 \theta_K + F_L \cos^2 \theta_K \right. \\ & + \frac{1}{4} (1 - F_L) \sin^2 \theta_K \cos 2\theta_l - F_L \cos^2 \theta_K \cos 2\theta_l \\ & + S_3 \sin^2 \theta_K \sin^2 \theta_l \cos 2\phi + S_4 \sin 2\theta_K \sin 2\theta_l \cos \phi \\ & + S_5 \sin 2\theta_K \sin \theta_l \cos \phi + S_6 \sin^2 \theta_K \cos \theta_l + S_7 \sin 2\theta_K \sin \theta_l \sin \phi \\ & \left. + S_8 \sin 2\theta_K \sin 2\theta_l \sin \phi + S_9 \sin^2 \theta_K \sin^2 \theta_l \sin 2\phi \right]. \end{aligned}$$

- In addition to  $F_L$ , we can measure the FF independent parameters.

$$P_i^{(s,c)} = \frac{S_i^{(s,c)}}{\sqrt{F_L(1 - F_L)}}$$

→ 9 observables to measure in total.

- Can reduce the number of observables directly by **folding** the differential decay rate and exploiting the symmetries in the angular expressions, e.g.:

$$\begin{aligned} \phi & \rightarrow -\phi \quad \text{if } \phi < 0 \\ \theta_l & \rightarrow \pi - \theta_l \quad \text{if } \theta_l > \frac{\pi}{2} \end{aligned}$$

- ✓ Complete information.
- ✓ FF independent observables at LO

# CP Asymmetry

---

- The CP asymmetry,  $A_{CP}$ , for  $B_d^0 \rightarrow K^{*0} \mu^+ \mu^-$  is defined as:

$$A_{CP} = \frac{\bar{N} - N}{\bar{N} + N}$$

- The data gives us:  $N_{obs} = (1 - \omega)N + \bar{\omega}\bar{N}$  and  $\bar{N}_{obs} = (1 - \bar{\omega})\bar{N} + \omega N$

- Hence:

$$A_{CP} = \frac{(1 - \Delta\omega)\bar{N}_{obs} - (1 + \Delta\omega)N_{obs}}{(1 - \bar{\omega} - \omega)(\bar{N}_{obs} + N_{obs})}$$

- $A_{CP}$  is predicted to be of the order  $<10^{-2}$  in the SM. [Christoph Bobeth et al JHEP07(2008)106]

- The measurement is sensitive to physics beyond the SM.

**$B^0_s \rightarrow \mu^+ \mu^-$  Back Up**

# $B_s^0 \rightarrow \mu^+ \mu^-$ Discriminating Variables

- Variables are listed in order of relevance as ranked by the multivariate classifier used in the final signal/background separation.

Variable	Description	Ranking
$L_{xy}$	Scalar product in the transverse plane of $(\Delta\vec{x} \cdot \vec{p}^B)/ \vec{p}_T^B $	1
$I_{0.7}$ isolation	Ratio of $ \vec{p}_T^B $ to the sum of $ \vec{p}_T^B $ and the transverse momenta of all tracks with $p_T > 0.5$ GeV within a cone $\Delta R < 0.7$ from the $B$ direction, excluding $B$ decay products	2
$ \alpha_{2D} $	Absolute value of the angle in the transverse plane between $\Delta\vec{x}$ and $\vec{p}^B$	3
$p_L^{\min}$	Minimum momentum of the two muon candidates along the $B$ direction	4
$p_T^B$	$B$ transverse momentum	5
$ct$ significance	Proper decay length $ct = L_{xy} \times m_B/p_T^B$ divided by its uncertainty	6
$\chi_z^2, \chi_{xy}^2$	Significance of the separation between production (PV) and decay vertex (SV) $\Delta\vec{x}^T \cdot (\sigma_{\Delta\vec{x}}^2)^{-1} \cdot \Delta\vec{x}$ , in $z$ and $(x, y)$ , respectively	7, 13
$ D_{xy} ^{\min},  D_z ^{\min}$	Absolute values of the minimum distance of closest approach in the $xy$ plane or along $z$ of tracks in the event to the $B$ vertex	8, 11
$\Delta R$	Angle $\sqrt{(\Delta\phi)^2 + (\Delta\eta)^2}$ between $\Delta\vec{x}$ and $\vec{p}^B$	9
$ d_0 ^{\max},  d_0 ^{\min}$	Absolute values of the maximum and minimum impact parameter in the transverse plane of the $B$ decay products relative to the primary vertex	10, 12



**$B_s^0 \rightarrow J/\psi \phi$  Back Up**

# Time-dependent amplitudes

$k$	$\mathcal{O}^{(k)}(t)$	$g^{(k)}(\theta_T, \psi_T, \phi_T)$
1	$\frac{1}{2}  A_0(0) ^2 [(1 + \cos \phi_s) e^{-\Gamma_L^{(s)} t} + (1 - \cos \phi_s) e^{-\Gamma_H^{(s)} t} \pm 2e^{-\Gamma_s t} \sin(\Delta m_s t) \sin \phi_s]$	$2 \cos^2 \psi_T (1 - \sin^2 \theta_T \cos^2 \phi_T)$
2	$\frac{1}{2}  A_{\parallel}(0) ^2 [(1 + \cos \phi_s) e^{-\Gamma_L^{(s)} t} + (1 - \cos \phi_s) e^{-\Gamma_H^{(s)} t} \pm 2e^{-\Gamma_s t} \sin(\Delta m_s t) \sin \phi_s]$	$\sin^2 \psi_T (1 - \sin^2 \theta_T \sin^2 \phi_T)$
3	$\frac{1}{2}  A_{\perp}(0) ^2 [(1 - \cos \phi_s) e^{-\Gamma_L^{(s)} t} + (1 + \cos \phi_s) e^{-\Gamma_H^{(s)} t} \mp 2e^{-\Gamma_s t} \sin(\Delta m_s t) \sin \phi_s]$	$\sin^2 \psi_T \sin^2 \theta_T$
4	$\frac{1}{2}  A_0(0)   A_{\parallel}(0)  \cos \delta_{\parallel}$ $[(1 + \cos \phi_s) e^{-\Gamma_L^{(s)} t} + (1 - \cos \phi_s) e^{-\Gamma_H^{(s)} t} \pm 2e^{-\Gamma_s t} \sin(\Delta m_s t) \sin \phi_s]$	$-\frac{1}{\sqrt{2}} \sin 2\psi_T \sin^2 \theta_T \sin 2\phi_T$
5	$ A_{\parallel}(0)   A_{\perp}(0)  [\frac{1}{2} (e^{-\Gamma_L^{(s)} t} - e^{-\Gamma_H^{(s)} t}) \cos(\delta_{\perp} - \delta_{\parallel}) \sin \phi_s$ $\pm e^{-\Gamma_s t} (\sin(\delta_{\perp} - \delta_{\parallel}) \cos(\Delta m_s t) - \cos(\delta_{\perp} - \delta_{\parallel}) \cos \phi_s \sin(\Delta m_s t))]$	$\sin^2 \psi_T \sin 2\theta_T \sin \phi_T$
6	$ A_0(0)   A_{\perp}(0)  [\frac{1}{2} (e^{-\Gamma_L^{(s)} t} - e^{-\Gamma_H^{(s)} t}) \cos \delta_{\perp} \sin \phi_s$ $\pm e^{-\Gamma_s t} (\sin \delta_{\perp} \cos(\Delta m_s t) - \cos \delta_{\perp} \cos \phi_s \sin(\Delta m_s t))]$	$\frac{1}{\sqrt{2}} \sin 2\psi_T \sin 2\theta_T \cos \phi_T$
7	$\frac{1}{2}  A_S(0) ^2 [(1 - \cos \phi_s) e^{-\Gamma_L^{(s)} t} + (1 + \cos \phi_s) e^{-\Gamma_H^{(s)} t} \mp 2e^{-\Gamma_s t} \sin(\Delta m_s t) \sin \phi_s]$	$\frac{2}{3} (1 - \sin^2 \theta_T \cos^2 \phi_T)$
8	$ A_S(0)   A_{\parallel}(0)  [\frac{1}{2} (e^{-\Gamma_L^{(s)} t} - e^{-\Gamma_H^{(s)} t}) \sin(\delta_{\parallel} - \delta_S) \sin \phi_s$ $\pm e^{-\Gamma_s t} (\cos(\delta_{\parallel} - \delta_S) \cos(\Delta m_s t) - \sin(\delta_{\parallel} - \delta_S) \cos \phi_s \sin(\Delta m_s t))]$	$\frac{1}{3} \sqrt{6} \sin \psi_T \sin^2 \theta_T \sin 2\phi_T$
9	$\frac{1}{2}  A_S(0)   A_{\perp}(0)  \sin(\delta_{\perp} - \delta_S)$ $[(1 - \cos \phi_s) e^{-\Gamma_L^{(s)} t} + (1 + \cos \phi_s) e^{-\Gamma_H^{(s)} t} \mp 2e^{-\Gamma_s t} \sin(\Delta m_s t) \sin \phi_s]$	$\frac{1}{3} \sqrt{6} \sin \psi_T \sin 2\theta_T \cos \phi_T$
10	$ A_0(0)   A_S(0)  [\frac{1}{2} (e^{-\Gamma_H^{(s)} t} - e^{-\Gamma_L^{(s)} t}) \sin \delta_S \sin \phi_s$ $\pm e^{-\Gamma_s t} (\cos \delta_S \cos(\Delta m_s t) + \sin \delta_S \cos \phi_s \sin(\Delta m_s t))]$	$\frac{4}{3} \sqrt{3} \cos \psi_T (1 - \sin^2 \theta_T \cos^2 \phi_T)$

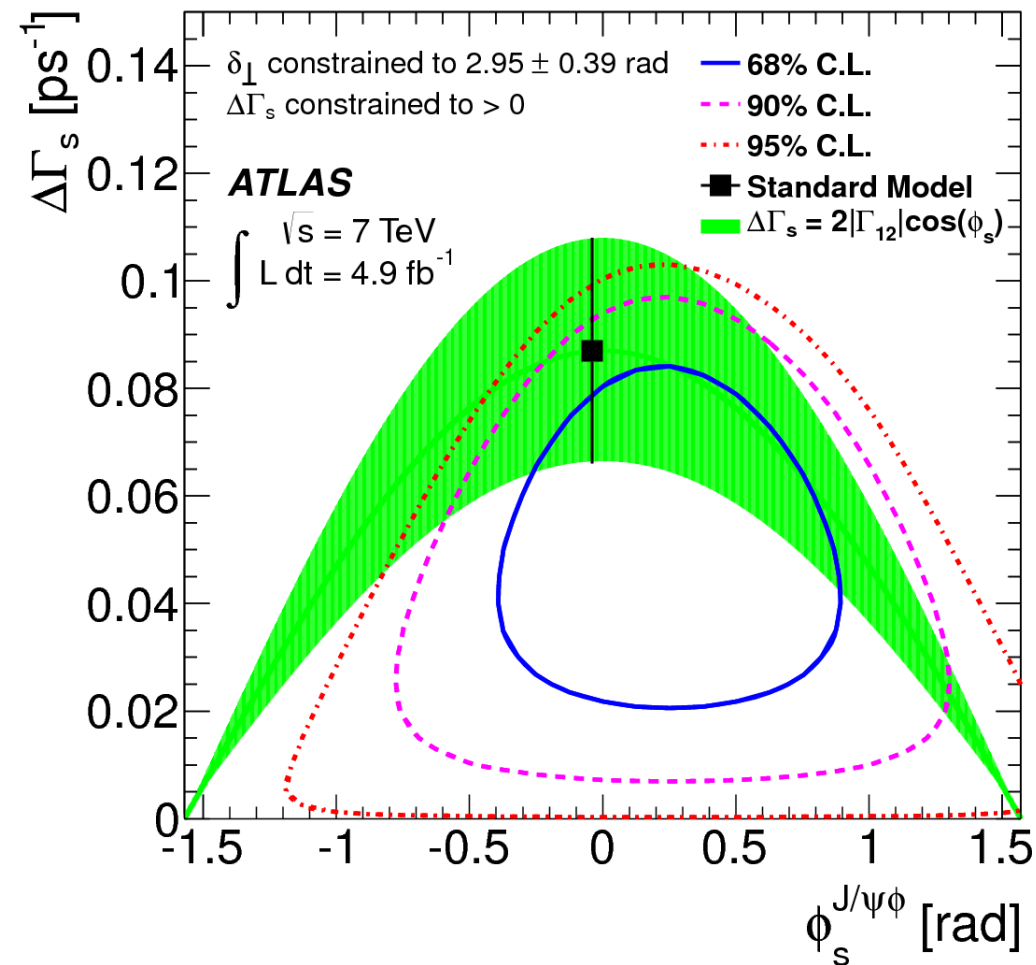
# Systematic Uncertainties

	$\phi_s$ [rad]	$\Delta\Gamma_s$ [ps <sup>-1</sup> ]	$\Gamma_s$ [ps <sup>-1</sup> ]	$ A_{\parallel}(0) ^2$	$ A_0(0) ^2$	$ A_S(0) ^2$	$\delta_{\perp}$ [rad]	$\delta_{\parallel}$ [rad]	$\delta_{\perp} - \delta_S$ [rad]
ID alignment	$<10^{-2}$	$<10^{-3}$	$<10^{-3}$	$<10^{-3}$	$<10^{-3}$	...	$<10^{-2}$	$<10^{-2}$	...
Trigger efficiency	$<10^{-2}$	$<10^{-3}$	0.002	$<10^{-3}$	$<10^{-3}$	$<10^{-3}$	$<10^{-2}$	$<10^{-2}$	$<10^{-2}$
$B^0$ contribution	0.03	0.001	$<10^{-3}$	$<10^{-3}$	0.005	0.001	0.02	$<10^{-2}$	$<10^{-2}$
Tagging	0.03	$<10^{-3}$	$<10^{-3}$	$<10^{-3}$	$<10^{-3}$	$<10^{-3}$	0.04	$<10^{-2}$	$<10^{-2}$
Acceptance	0.02	0.004	0.002	0.002	0.004	...	...	$<10^{-2}$	...
Models:									
Default fit	$<10^{-2}$	0.003	$<10^{-3}$	0.001	0.001	0.006	0.07	0.01	0.01
Signal mass	$<10^{-2}$	0.001	$<10^{-3}$	$<10^{-3}$	0.001	$<10^{-3}$	0.03	0.04	0.01
Background mass	$<10^{-2}$	0.001	0.001	$<10^{-3}$	$<10^{-3}$	0.002	0.06	0.02	0.02
Resolution	0.02	$<10^{-3}$	0.001	0.001	$<10^{-3}$	0.002	0.04	0.02	0.01
Background time	0.01	0.001	$<10^{-3}$	0.001	$<10^{-3}$	0.002	0.01	0.02	0.02
Background angles	0.02	0.008	0.002	0.008	0.009	0.027	0.06	0.07	0.03
Total	0.05	0.010	0.004	0.009	0.012	0.028	0.11	0.09	0.04

# Tagged and untagged 2011 analysis

## Untagged

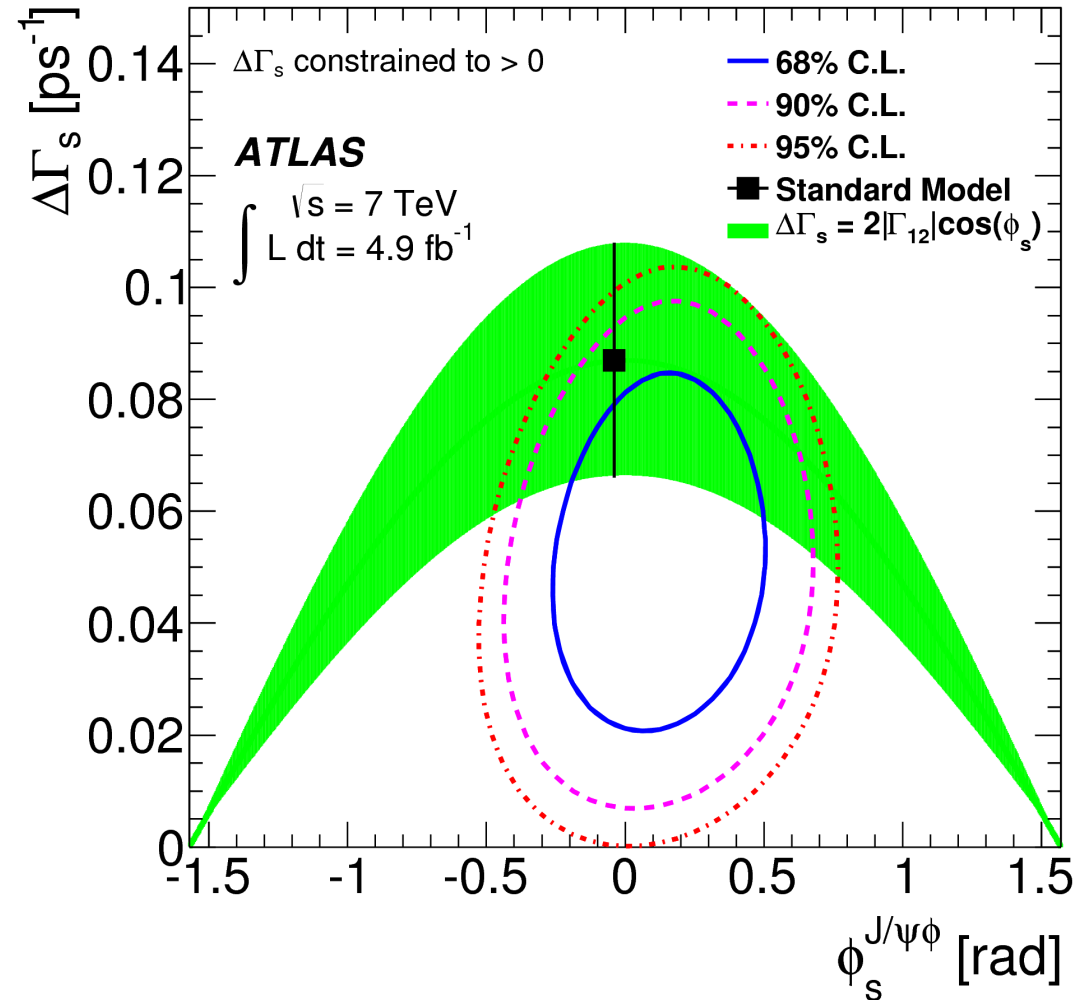
[JHEP 1212 (2012) 072]



## Tagged

[JHEP 1212 (2012) 072]

40% better  $\phi_s$  stat. error,  
 $\Delta\Gamma_s$  error unchanged

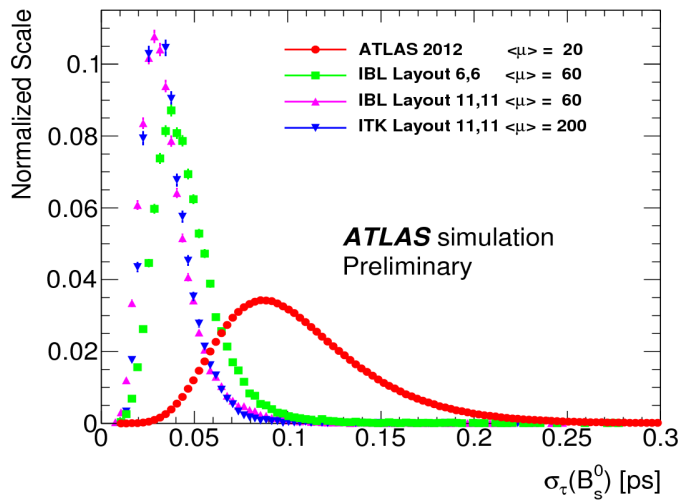
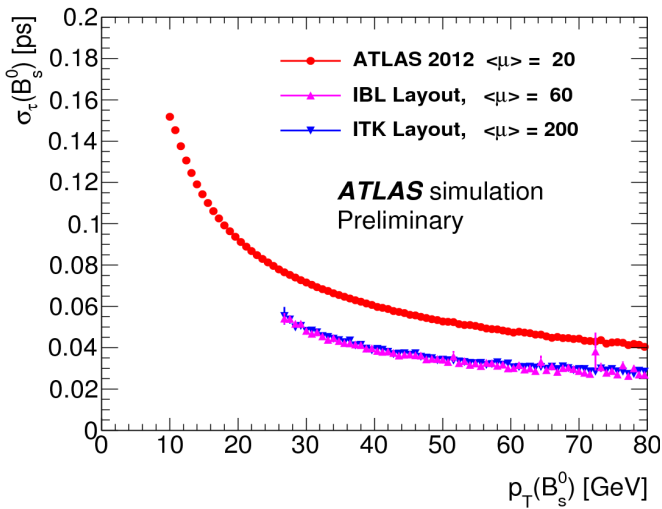


# Case Study – CPV in $B_s \rightarrow J/\psi \phi$ at ATLAS

ATLAS-PHYS-PUB-2013-010

- Time-dependent angular analysis of the  $B_s \rightarrow J/\psi(\mu^+\mu^-) \phi(K^+K^-)$  decays
- Key factors: # of signal candidates, lifetime precision, performance stability in high pileup

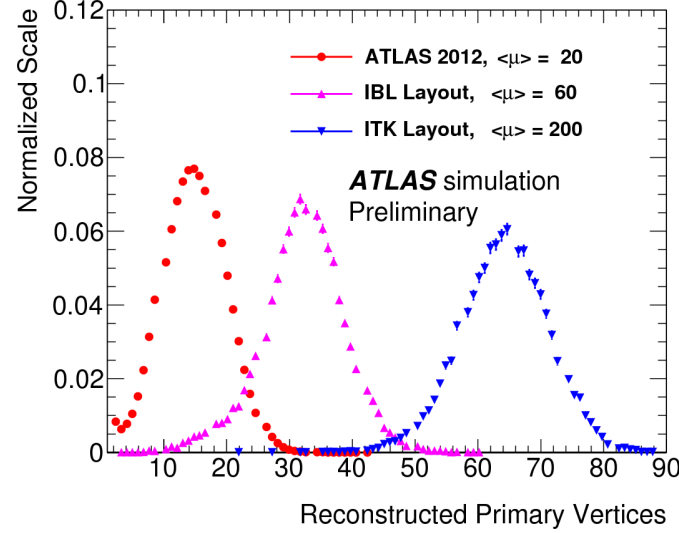
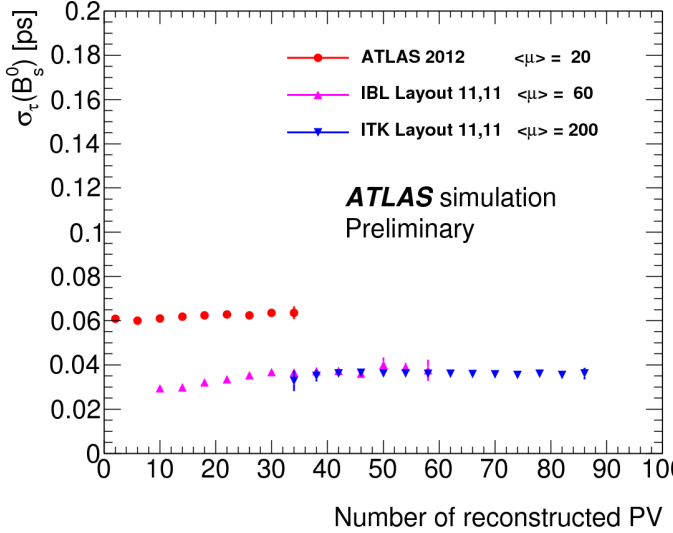
## Lifetime precisions:



- New ID layouts IBL and ITK **improve** proper decay time resolution  $\sigma_\tau$  **by 30%** w.r.t. Run-1

- Higher  $p_T$  improves  $\sigma_\tau$  and signal purity on the account of lower efficiency

## Stability with # of primary vertices:



- Resolution  $\sigma_\tau$  (secondary vertex displacement from PV) may deteriorate with increasing #PV (select correct PV based on  $B_s$ -momentum direction)

- $\sigma_\tau$  stable in Run-1 (low- $p_T$ , dominated by material)

- Slight  $\sigma_\tau$  (~14%) increase in Run-2 with #PV, **stable** at #PV > 40

# Case Study – CPV in $B_s \rightarrow J/\psi\phi$ at ATLAS

- Trigger scenario: di-muon with the muon  $p_T$  thresholds:
  - **Run-2/3:** 6+6 GeV (nominal, assuming basic L1-topo usage) or 11+11 GeV (pessimistic)
  - **HI-LHC:** 11+11 GeV

	2011	2012	2015-17		2019-21	2023-30+
Detector	current	current	IBL		IBL	ITK
Average interactions per BX $\langle\mu\rangle$	6-12	21	60		60	200
Luminosity, $\text{fb}^{-1}$	4.9	20	100		250	3 000
Di- $\mu$ trigger $p_T$ thresholds, GeV	4 - 4(6)	4 - 6	6 - 6	11 - 11	11 - 11	11 - 11
Signal events per $\text{fb}^{-1}$	4 400	4 320	3 280	460	460	330
Signal events	22 000	86 400	327 900	45 500	114 000	810 000
Total events in analysis	130 000	550 000	1 874 000	284 000	758 000	6 461 000
MC $\sigma(\phi_s)$ (stat.), rad	0.25	0.12	0.054	0.10	0.064	0.022

- Toy-MC prediction based on 2011 analysis, 2012 sidebands data and fully simulated signal at Run-2/3/HL-LHC conditions
- Potential in Runs-2/3 will strongly depend on the trigger thresholds:  $\sim 7x$  less  $B_s$  events in the pessimistic 11+11 GeV  $p_T(\mu^\pm)$  trigger configuration
- Results prepared for ECFA 2013 (ATL-PHYS-PUB-2013-010), considered conservative:
  - Further development of the L1-topological usage => part of the Run-2 data expected to be collected by triggers with lower muon  $p_T$  thresholds: 4-6 GeV
  - (Not considered flavour tagging and fit improvements developed in analysis of 8 TeV data of 2012)